SEMARAK ILMU PUBLISHING

Semarak International Journal of Electronic System Engineering

Journal homepage:
https://semarakilmu.com.my/journals/index.php/sijese/index
ISSN: 3030-5519

3-D Printed Antennas with Dielectric Lens for Free-Space Constitutive Parameters Measurement

Renukka SIvakumar[1,*], Saidatul Norlyana Azemi[2], Lee Yeng Seng[3], Kok Yeow You[4], Ping Jack Soh[5]

[1] Faculty of Electronic Engineering Technology, Universiti Malaysia Perlis, Kampus Alam Unimap Pauh Putra,02600, Arau, Perlis, Malaysia
[2] Advanced Communication Engineering, Centre of Excellence (COE), Universiti Malaysia Perlis, Puah, Malaysia
[3] School of Computer and Communication Engineering, Universiti Malaysia Perlis (UniMAP), Pauh Putra Campus, Arau, Perlis 02600, Malaysia
[4] Faculty of Electrical Engineering, Universiti Teknologi Malaysia, 81310, UTM, Skudai, Johor, Malaysia
[5] Centre of Wireless Communications (CWC), University of Oulu, 90570, Oulu, Finland

ARTICLE INFO

Article history:
Received 20 January 2024
Received in revised form 14 February 2024
Accepted 2 March 2024
Available online 30 March 2024

Keywords:
Free-space; K-band; Ka-band; 3-D printing

ABSTRACT

Over the last two decades, mm-wave and terahertz (THz) technologies have advanced significantly, owing to their appealing properties in a variety of applications such as automotive paint materials, metamaterial structures, radio astronomy, the military, and medicine. Researchers have investigated various metamaterial structures to determine their permeability. The free-space measurement technique is widely used to determine the electrical properties of materials. The free-space measurement approach has gained popularity because it allows for more efficient measurements at higher millimetre-wave and terahertz frequencies. This is primarily due to its ease of use, non-destructive features, and ability to perform reflection and transmission measurements without interacting physically with the sample. The goal of this research is to create a free space material measurement system that can accurately determine permeability and permittivity. A software based on a modified NRW algorithm was developed to determine the permeability and permittivity of materials with high accuracy. High gain K-band and Ka-band horn antennas from 18 GHz to 39 GHz were designed using 3D printing technology to eliminate the need for the commercial measurement systems. To reduce measurement inaccuracies, a 3-D printed dielectric lens was designed and fabricated using 3-D printing technology, with the beam focus of the antenna optimized. 3-D printed horn antennas performed similarly to commercial horn antennas in terms of S11, gain, and 3-dB beamwidth. Furthermore, the permeability and permittivity of MUTs were determined with high accuracy using the software for the commercial horn antennas and 3-D printed horn antennas.

1. Introduction

The characterization of dielectric materials plays a crucial role in understanding their properties. Having knowledge about dielectric properties in our everyday lives helps us comprehend how foods behave during microwave heating, how liquids function as dielectrics in transformers, and how they serve as insulating layers in Printed Circuit Board (PCB) build-up. These examples highlight the

* *Corresponding author.*
E-mail address: renukkasivakumar@gmail.com

significance of dielectric properties in our daily experiences. In the last twenty years, there has been a significant and intensive development of millimetre wave (mm-wave) and terahertz (THz) technologies. These advancements are attributed to their appealing properties, which find practical applications in various fields, including radio astronomy and military applications.

The increasing demands for mm-wave components and systems created a renewed need for cost-effective test and measurement solutions within this band and beyond. One of the important steps in designing devices operating at these frequencies is to first determine the electrical properties of materials. These values affect the method to design various radio components, as their behaviour varies according to frequency. This need arises as most materials are typically characterized up to the microwave bands. Besides that, material characterization can also be applied to determine quality of agricultural and industrial products, and biomedical applications [1].

Various measurement techniques have been established to determine material characteristics, specifically dielectric properties in terms of permittivity and permeability at microwave frequencies. These techniques include the free space method, transmission line method, waveguide method, impedance, coaxial probe, and cavity methods [2-7]. Among these techniques, the free space measurement technique is popular as it allows the measurement of reflection and transmission measurements without any physical contact with the sample [8-10]. This method is particularly well-suited for thin, flat-faced materials or other substances that can be shaped accordingly. With the increasing demand for efficient, accurate, broadband material measurement systems utilizing higher mm-wave and THz frequencies. The renewed interest in the free-space measurement method stems from the increasing demand for new applications that necessitate efficient, accurate, and broadband material measurement systems operating at higher mm-wave and THz frequencies. Among the different types of measurement techniques, free space is preferred as it can use for high frequency measurements. Figure 1 shows the applications of dielectric properties. One of it, is determining the behaviour of foods during microwave heating. Also, liquid dielectric in transformers and insulating layer in the PCB build up are other applications of dielectric in our daily life.

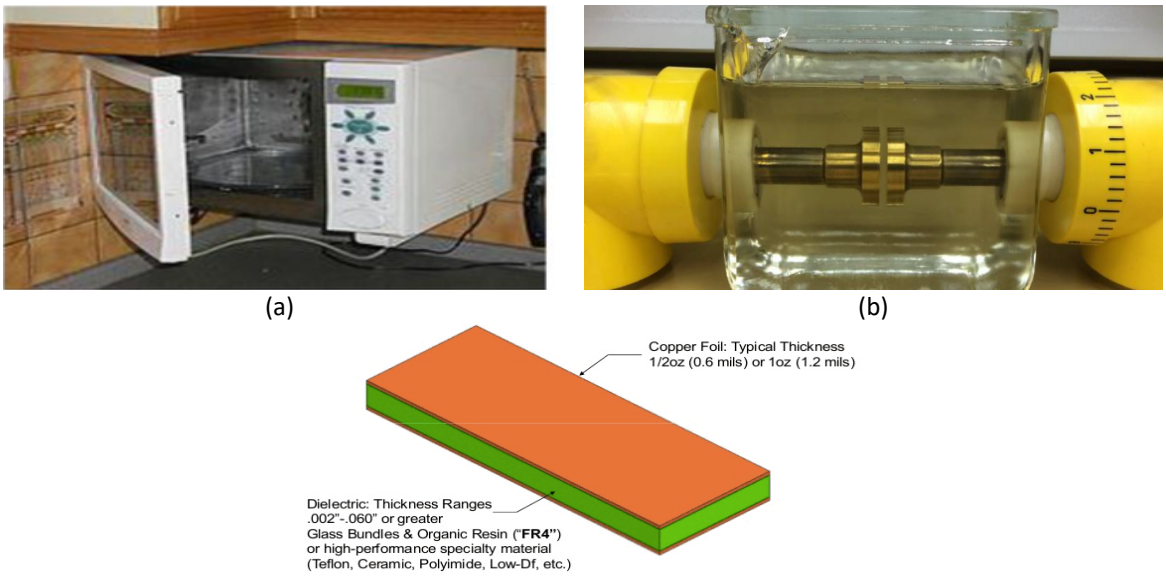

(a) (b)

(c)

Fig. 1. Applications of dielectric properties. (a) Microwave heating [11](b) Liquid dielectric in transformer [12] (c) As an insulating layer in PCB build up [13]

One of the biggest problems small machinists and startups have that is, CNC machines are quite expensive, which prevents them from being customised. Since 3D printing was used to create most of the machine's components, the user can alter the apparatus to suit their needs. Most of the machine's parts were made with affordable 3D printing technology. Because of its energy efficiency, low post-processing waste, ease of fabrication, low human engagement, simplicity, adaptability, and minimal material waste, 3D printing is a sustainable technology for industrial use. For determination of dielectric properties of materials, most of the studies focused on modifying the conversion algorithms such as NRW algorithm rather than develop a software program that could determine dielectric properties with high precision. Also, the algorithms could not determine both the permeability and permittivity of a material. This research concentrates on software program that utilizes the modified NRW algorithm to accurately determine the permeability and permittivity of materials with high precision. In this research, the complete system, consisting of the antennas, focusing mechanism, and MUT, is simulated using appropriate software. The simple software program, enable the determination of the MUT s' permeability and permittivity with high accuracy.

This paper aims to reevaluate dielectric material characterization with the free space method, particularly concentrating on its extension towards higher frequencies for the 3-D printed antennas with dielectric lens for free-space constitutive parameters measurement. Initially, the paper provides an overview of the 3-D printed horn antennas, dielectric lens designs and specifications. Additionally, it discusses the results obtained for the 3-Dprinted horn antennas and commercial horn antennas. The paper also provides the results from the software that determines the permeability and permittivity of the MUTs.

2. 3-D Printing

Machining of horn antennas requires use of 4-dimension Computer Numerical Control (CNC) which is more difficult. The high cost of CNC machines is a major issue that small machinists and startups face, and it also makes them unsuitable for customisation. The majority of this machine's components were produced via 3D printing, enabling the user to modify the device to meet different demands [14-16]. Majority of the machine's components were created using cost-effective 3D printing technology. 3D printing is a sustainable technology for industrial application because of its energy efficiency, low post-processing waste, ease of manufacture, low human participation, simplicity, flexibility and minimal material waste [17].

2.1 3-D Printed Horn Antennas and Dielectric Lens

The 1st phase of this project was to design 3-D printed circular horn antennas for K-band and Ka-band, which operate within the frequency ranges of 18 GHz to 26 GHz and 26 GHz to 39 GHz, respectively, for a free-space material measurement system. Table 1 and 2 detail the dimensions and specifications of the K-band horn antenna. These horn antennas were designed and simulated using CST Microwave Studio Suite. Figure 2 illustrates the dimensions of the proposed K-band horn antenna. Table 1 presents the specifications for the K-band horn antenna, designed for the frequency range of 18 GHz to 26 GHz, with a gain of 11.5dBi to 15.5dBi. The reflection coefficient measured was consistently below -10 dB, and the radiation pattern exhibited a directional nature. Moreover, the radiation efficiency ranged from 98% to 99%, with the total efficiency falling between 96% and 99%. It's worth noting that these K-band horn antenna specifications closely mirrored those of the commercial horn antenna.

Table 1
K-band Horn Antenna Specifications

Antenna Specifications	3-D Printed Specification	Commercial Horn Specification
Frequency range	18 GHz to 26 GHz	18 GHz to 40 GHz
Antenna type	Horn antenna	Horn antenna
Gain	11.5 dBi-15.5 dBi	13 dBi-16 dBi
Reflection Coefficient	Below -10 dB	Below -10 dB
Radiation	Directional	Directional
Radiation efficiency	98 % to 99 %	-
Total efficiency	96% to 99 %	-

Table 2
K-band Horn Antenna Dimensions

Parameters	Values (mm)
Horn flare diameter, H	30
Antenna thickness, T	2
Horn flare length, L	40
Waveguide width, W_g	10.67
Waveguide height, W_h	4.32
Distance of pin, P	4

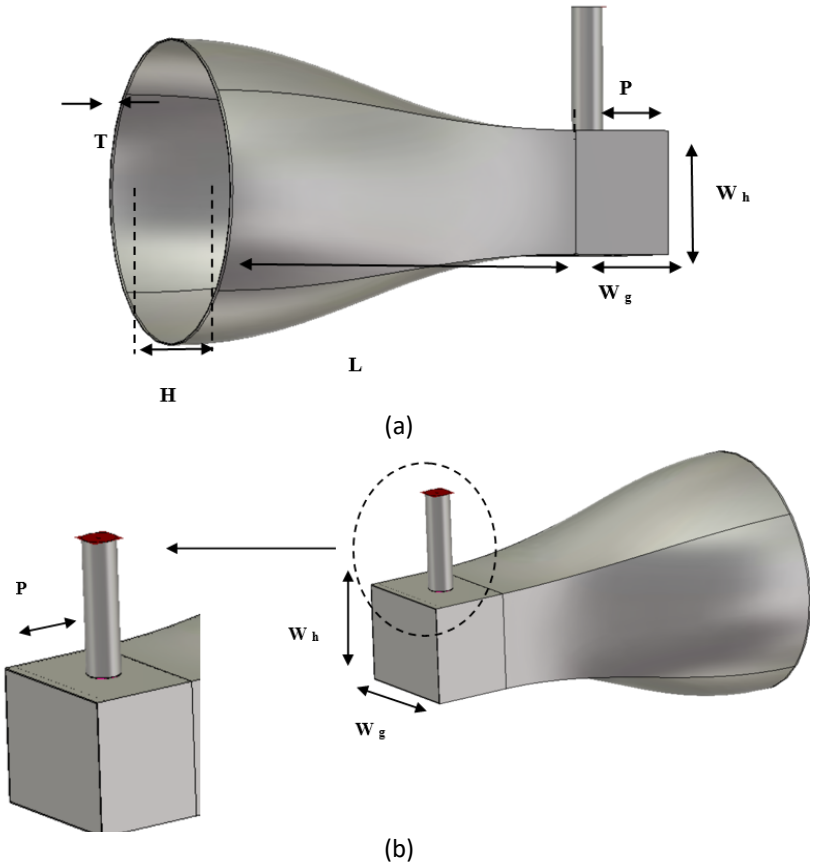

Fig. 2. (a) Dimensions of the proposed K-band antenna (b) Distance of pin from the waveguide and horn antenna side view

The choice of the K-band frequency for this dissertation is motivated by its suitability for various applications, including short-range communication, blind spot monitoring systems, automatic door openers, and accident prevention systems in automobiles. Additionally, the K-band frequency finds application in high-resolution, close-range targeting radars, military aircraft, space telescopes,

wireless point-to-point microwave communication systems, vehicle speed detection systems, and satellite communications, particularly in the Ka-band frequency range. These frequency ranges, K-band and Ka-band have proven valuable in satellite communication, telecommunications, and radio astronomy applications, which serve as the primary rationale for their selection as the focus of this dissertation.

Figure 3 shows the cutting plane of the K-band horn antenna and its coaxial part. Coaxial part consists of dielectric which is the Teflon, inner conductor, and the outer conductor. Table 3, presented below, provides a comprehensive overview of the parameters relevant to the design of a K-band horn antenna, spanning from 18 GHz to 26 GHz. This data will play a crucial role in the subsequent chapters of the dissertation, where the design and performance of such antennas will be explored and analysed in greater detail.

Table 3
K-band Horn Antenna Parameters

Parameters	Value (mm)
Radius of inner conductor (pin)	0.25
Radius of the dielectric (Teflon)	1.5
Radius of outer conductor	1.55
Length of the inner conductor	15
Length of dielectric (Teflon)	12
Length of outer conductor	12

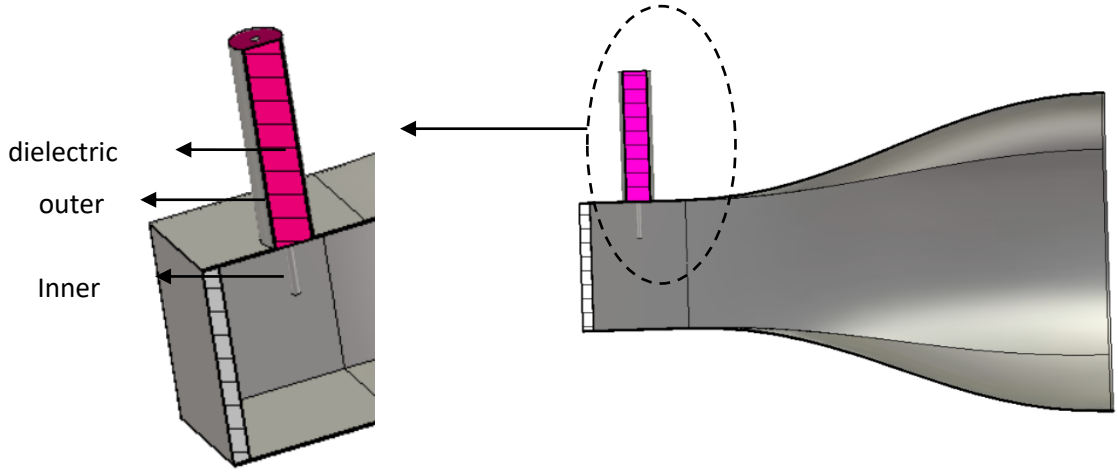

Fig. 3. Cutting plane diagram of the K-band horn antenna

Figure 4 displays the dimensions of the proposed Ka-band horn antenna, offering a visual insight into the physical configuration of the antenna. This illustrative representation offers a visual insight into the physical configuration of the antenna, enhancing our understanding of its structure and design. This figure will be referenced throughout the dissertation to aid in the explanation and analysis of the antenna's performance and functionality. Ka-band horn antenna specifications and dimensions are tabulated in Table 4 and 5.

Table 4
Ka-band Horn Antenna Specifications

Antenna Specifications	Value
Frequency range	26 GHz to 39 GHz
Antenna type	Horn antenna
Gain	12 dBi-15.5 dBi
Reflection Coefficient	Below -10 dB
Radiation	Directional
Radiation efficiency	88 % to 95 %
Total efficiency	85 % to 95 %

Table 5
K-band Horn Antenna Dimensions

Parameters	Values (mm)
Horn flare diameter, H	40
Antenna thickness, T	3
Horn flare length, L	30
Waveguide width, W_g	7.11
Waveguide height, W_h	3.56
Distance of pin, P	3

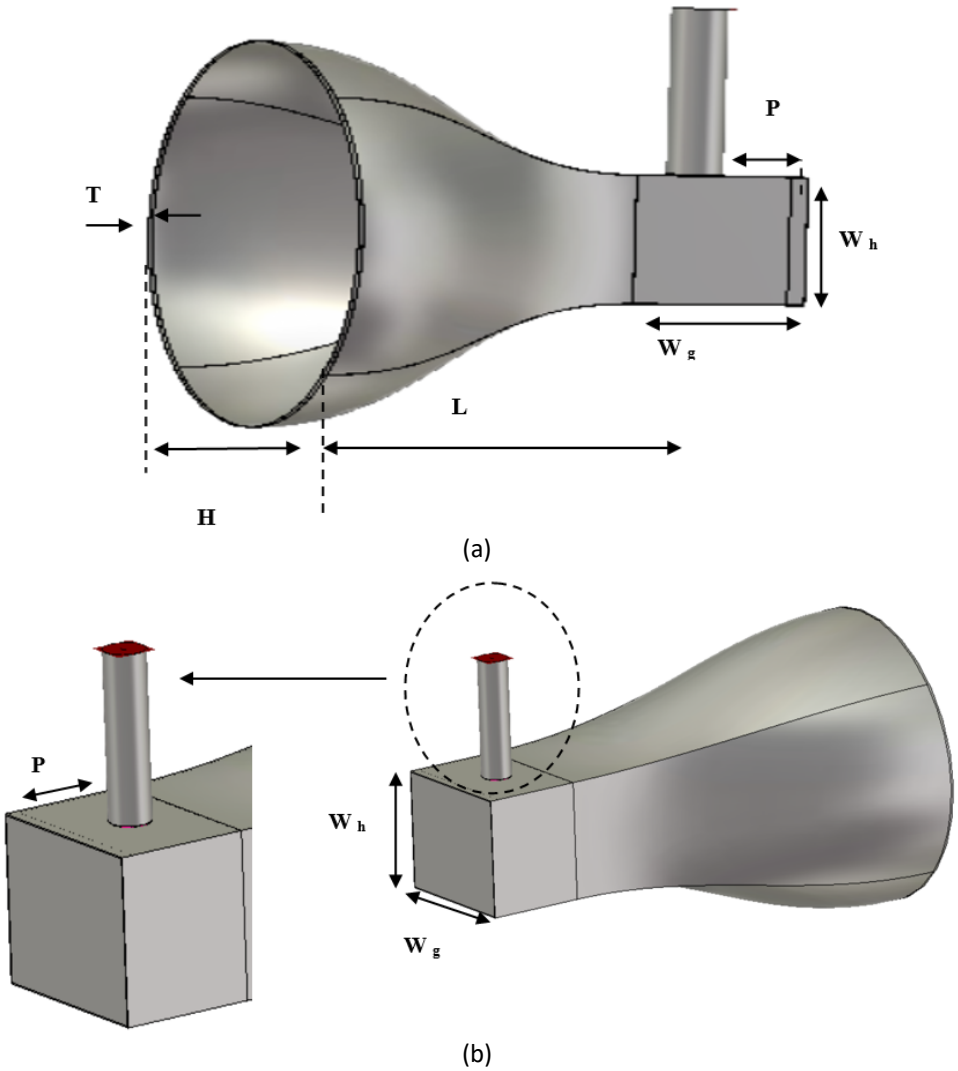

Fig. 4. (a) Dimensions of the proposed Ka-band antenna (b) Distance of pin from the waveguide and horn antenna side view

The design of dielectric lens was done in CST to evaluate the performance of the lens after the simulation. The dielectric lens of 4 mm thickness and r, radius of 4 cm was designed for the K-band antenna and dielectric lens of 6 mm thickness and radius of 5 cm was designed for the Ka-band antenna. This is because, as the horn flare diameter increases, the lens thickness and radius should be big enough to focus the beam onto the MUT for accurate determination of materials' permeability and permittivity. Then, the simulation result with or without lens was evaluated. Figure 5 and Figure 6 shows the front view and side view of the dielectric lens and design of lens in CST.

In order to fabricate, dielectric lens designed in CST was sliced in Creality Slicer, software to proceed with the 3D printing process as shown in Figure 7. The 3D printing was done with ABS material with 0.4mm nozzle size and printing temperature of 230°C. The infill density of the lens is 70% and the duration of the printing time is 4 hrs 16 minutes.

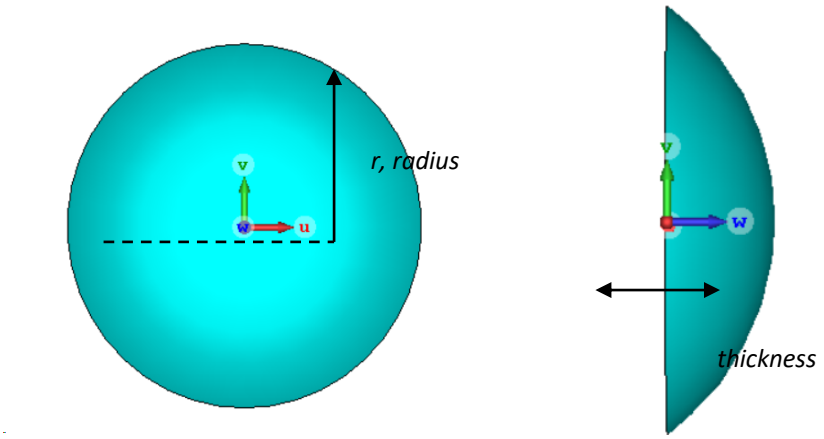

Fig. 5. Dielectric lens (a) Front view of lens (b) Side view of lens

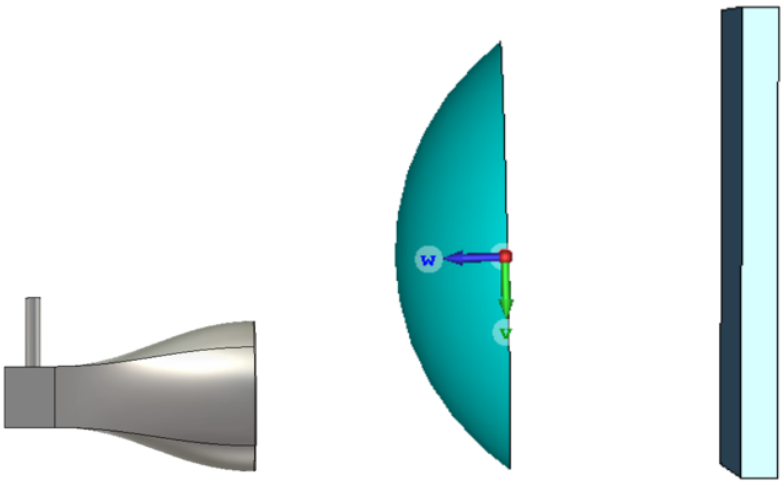

(a) (b) (c)

Fig. 6. Dielectric lens in CST (a) Horn antenna (b) Dielectric lens (c) Material Under Test

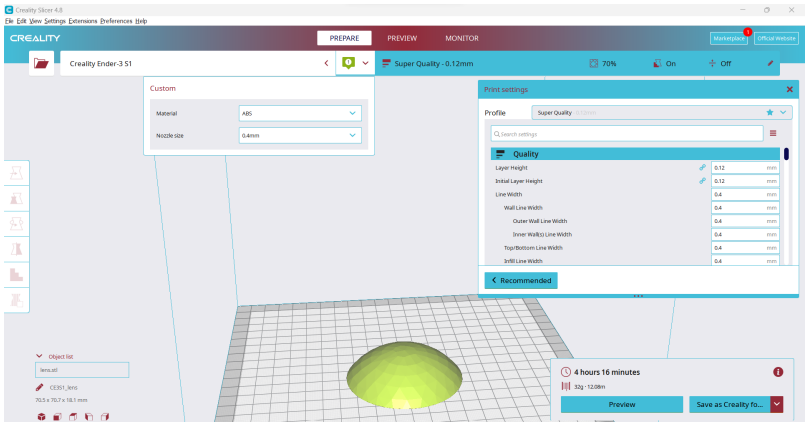

Fig. 7. Design of Dielectric lens in Creality Slicer

In this work, a 3-D printed dielectric lens was designed to enhance the gain of the horn antenna and to overcome limitations such as diffraction effects and limited operating range. Acrylonitrile butadiene styrene (ABS) lens was fabricated using fused deposition modelling (FDM) and the impact of dielectric lens has been studied by simulation in CST Studio Suite. The 3-D printing process was carried out using Creality Ender-3S1 as shown in Figure 8 below. Figure 9 and Figure 10 shows the 3-D printed dielectric lens and 3-D printed horn antennas.

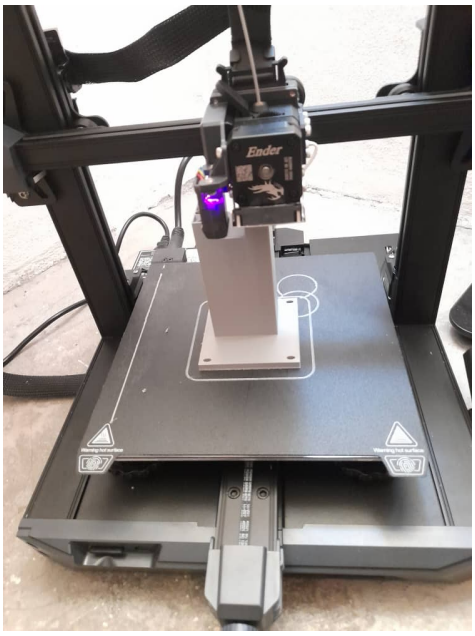

Fig. 8. 3-D printing process

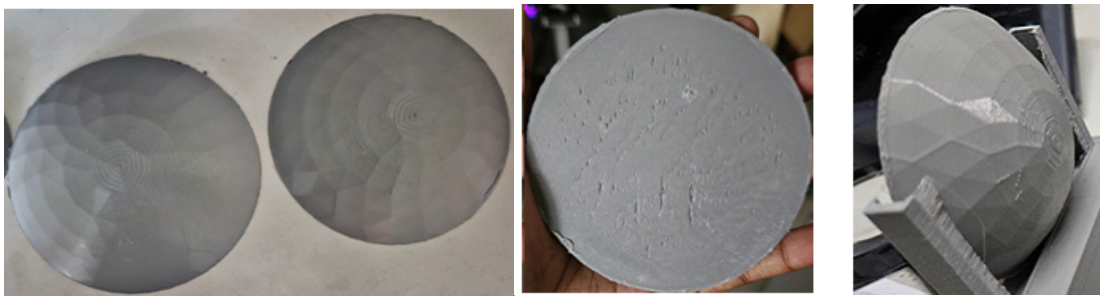

(a) (b) (c)

Fig. 9. 3-D printed dielectric lens (a) Front view (b) Back view (c) Side view

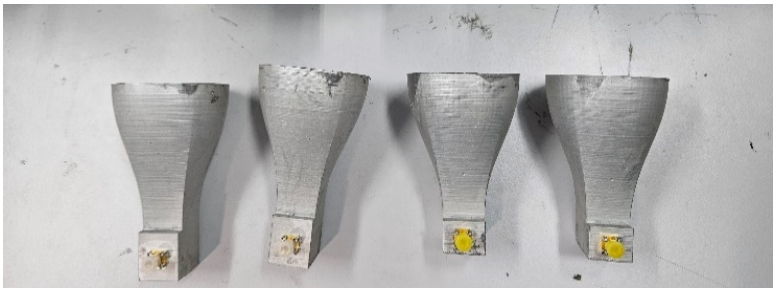

Fig. 10. 3-D printed horn antennas

3. Experimental Set-Up

The experimental setup for free space measurements encompasses a comprehensive arrangement of essential components aimed at meticulously examining the electromagnetic properties of samples under investigation. This setup is composed of a Vector Network Analyzer (VNA), meticulously chosen K-band and Ka-band horn antennas, as well as commercially available horn antennas, each serving a specific role in the measurement process. The VNA stands as the centre piece of the configuration, offering precise analysis of the electrical attributes of high-frequency elements, particularly antennas. Employing K-band and Ka-band horn antennas permits focused signal transmission and reception within their respective frequency bands, facilitating accurate data collection.

Central to the measurement setup is the inclusion of samples under test, serving as the focal point of the investigation. These samples are subjected to controlled electromagnetic waves emitted by the horn antennas, enabling the observation and recording of their intricate interactions with these waves. The experimental procedure is seamlessly orchestrated through the integration of a dedicated software program, streamlining the data acquisition process and offering potential avenues for in-depth analysis.

Furthermore, the configuration is visually delineated through Figure 11 and Figure 12, which provide graphical representations of the measurement setup. Figure 11 portrays the setup devoid of any additional optical components, offering a clear depiction of the core arrangement. In contrast, Figure 11 showcases the same measurement setup, albeit augmented with and without the presence of a lens. Figure 12 presents the measurement setup of 3-D printed horns with lens. These visual aids serve as essential references, aiding in the comprehension of the experimental apparatus and its variations.

In essence, the described free space measurement setup represents a meticulously designed and orchestrated arrangement, harmonizing cutting-edge hardware like the VNA and specialized horn antennas with software control and visualization through graphical representations. This configuration serves as a critical tool for in-depth exploration of the electromagnetic characteristics of the samples under scrutiny, contributing valuable insights to the broader field of electromagnetic research.

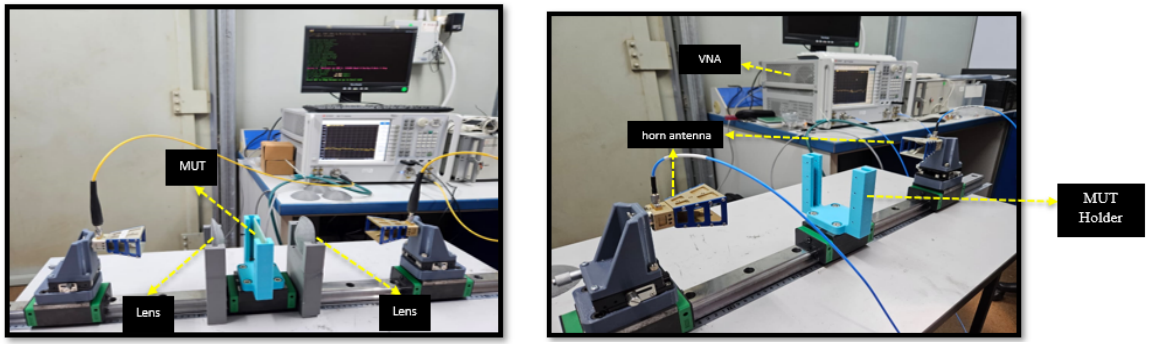

(a) (b)

Fig. 11. (a) measurement set-up with lens (b) Measurement set-up without lens

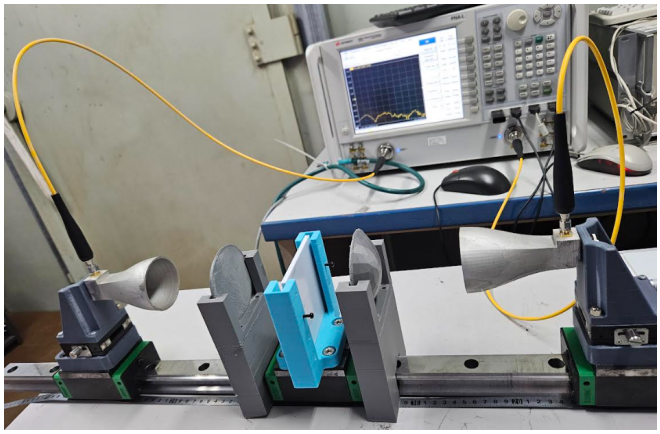

Fig. 12. Measurement setup with lens for 3-D printed horns

4. Results & Discussions

4.1 K-band, Ka-band and Commercial Horn Antenna Results & Discussions

The K-band and Ka-band horn antennas were designed using CST Studio suite and were 3-D printed. After the 3D printing process, the antennas were coated with silver coating paint to proceed with measurement process. In this section, 3-D printed K-band horn antenna results with and without lens and commercial horn antenna results with and without lens from 18 GHz to 39 GHz will be analysed.

Figure 13 below shows the S_{11} simulation and measurement results with and without lens for K-band horn antenna and commercial horn antenna. The simulated S_{11} results shows a good agreement with the measured S_{11} results. From 18 GHz to 26 GHz without the use of lens, the S_{11} simulation results is below -10 dB while for the measurement results the S_{11} is below -12 dB at throughout the frequency range. From 18 GHz to 26 GHz with the use of lens, the S_{11} simulation results is below -10 dB while for the measurement results the S_{11} is below -8 dB at throughout the frequency range. For the commercial horn antenna, measured S_{11} was better without the use of lens. For the pyramidal horn antenna, the simulated S_{11} was not good which results in design of circular horn antenna as reported in previous chapter. With, the use of dielectric lens, the return loss was degraded for the measurement and simulation results when compared with the return loss without the use of lens. Use of lens allows narrowed beamwidth which focus signals in particular direction throughout the K-band frequency range by converting the spherical waves to plane waves. As can be seen from the Figure 13, S_{11} below -10 dB was obtained for the 3-D printed horn antenna for K-band which showed a good agreement with S_{11} acquired by the commercial horn antenna.

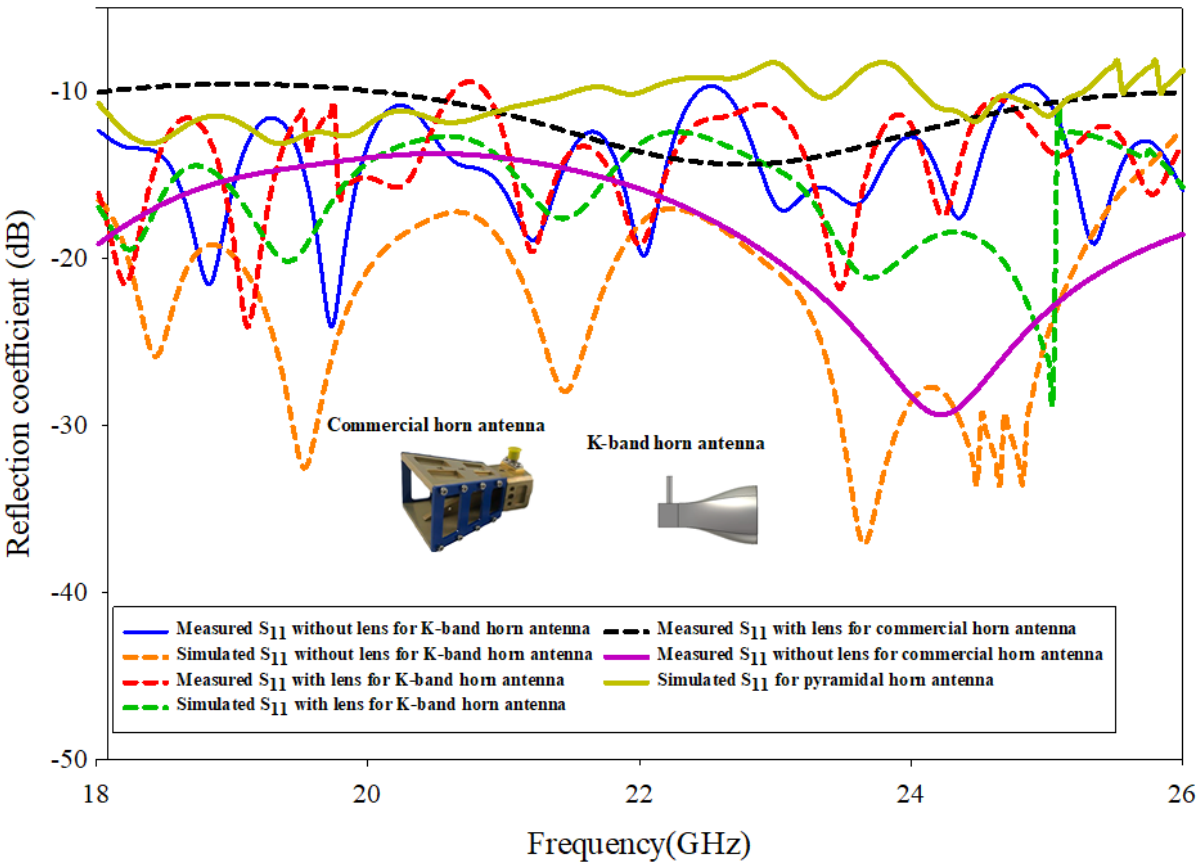

Fig. 13. S_{11} simulation results and measurement results for K-band antenna

Figure 14 below shows the S_{11} simulation and measurement results with and without lens for Ka-band horn antenna and commercial horn antenna. The simulated S_{11} results shows a good agreement with the measured S_{11} results. From 26 GHz to 39 GHz without the use of lens, the S_{11} simulation results is below -5 dB for certain frequency range while for the measurement results the S_{11} is below -10 dB at throughout the frequency range. From 26 GHz to 39 GHz with the use of lens, the S_{11} simulation results is below -10 dB for some operating frequency range while for the measurement results the S_{11} is below -10 dB at throughout the frequency range. For the commercial horn antenna, measured S_{11} was better without the use of lens. For the pyramidal horn antenna, the simulated S_{11} was not good which results in design of circular horn antenna as reported in previous chapter. With, the use of dielectric lens, the return loss was degraded for the measurement and simulation results when compared with the return loss without the use of lens. Use of lens allows narrowed beamwidth which focus signals in particular direction throughout the Ka-band frequency range by converting the spherical waves to plane waves. As can be seen from the Figure 14, S_{11} below -10 dB was obtained for the 3-D printed horn antenna for Ka-band which showed a good agreement with S_{11} acquired by the commercial horn antenna.

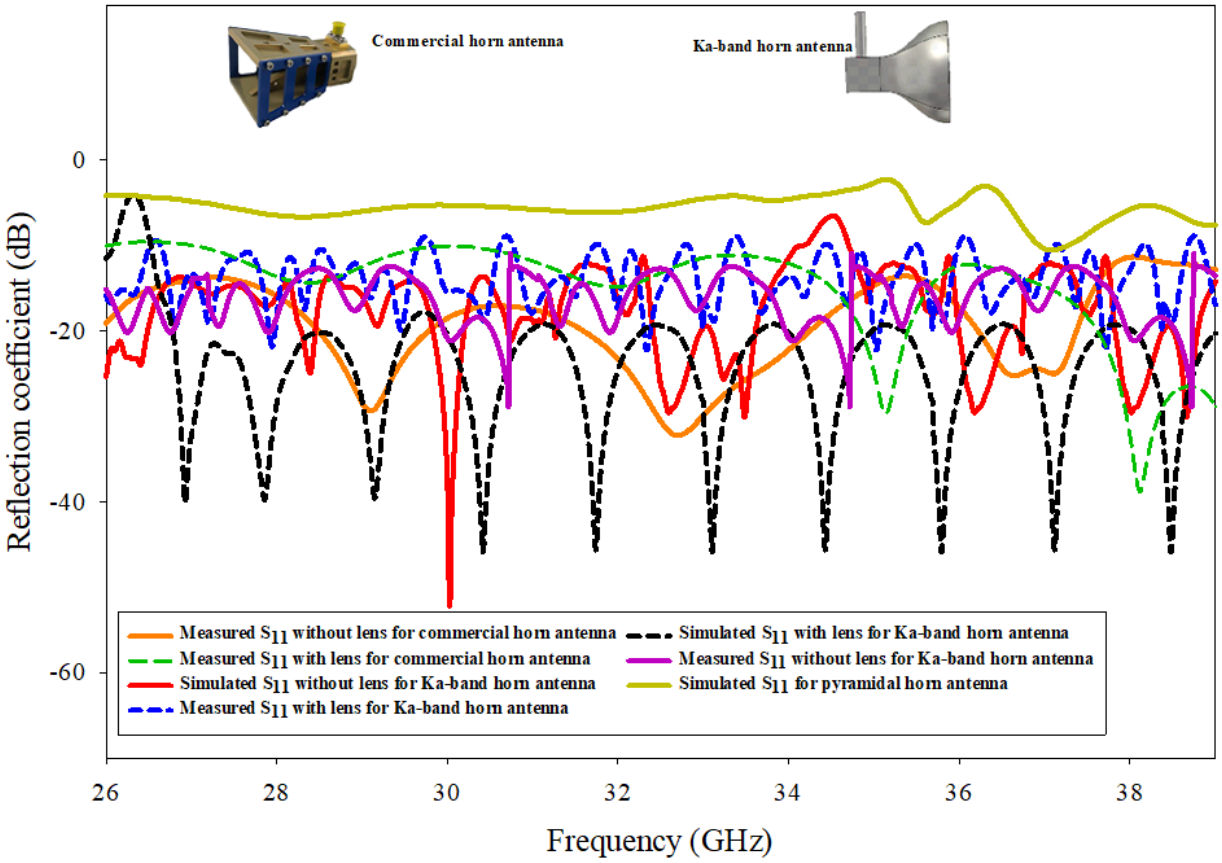

Fig. 14. S_{11} simulation results and measurement results for Ka-band antenna

4.2 Comparison Of 3- Db Beamwidth For 3-D Printed Horn Antennas and Commercial Horn Antenna

3- dB beamwidth results were compared for the 3-D printed horn antennas for K-band, Ka-band and commercial horn antenna with and without lens. For the K-band, Ka-band and commercial horn antenna in Figure 15, the 3- dB beamwidth is higher without the use of lens compared to the 3- dB beamwidth with lens. As for the 3- dB beamwidth, there is a difference of 10º to 30º between the commercial horn antenna and K-band and Ka-band horn antennas as shown in Figure 15. The use of lens narrowed the beamwidth throughout the frequency range by decreasing the 3- dB beamwidth.

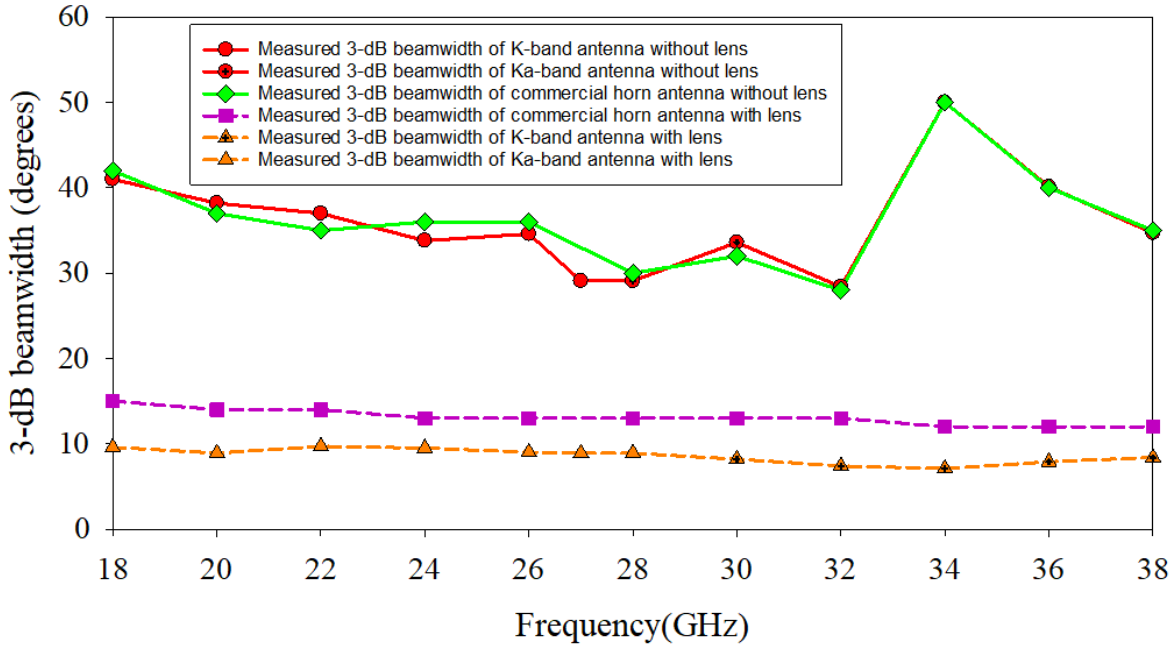

Fig. 15. 3- dB beamwidth of K-band antenna with and without lens

4.3 Comparison of Gain For 3-D Printed Horn Antennas and Commercial Horn Antenna

With the use of lens, the gain increased up to a maximum gain of 25.7 dBi when compared with the gain without the use of lens for the K-band horn antenna as shown in Figure 16. For the gain, the commercial horn antenna without lens acquired gain which is between the range of 13 dBi to 16 dBi as in Figure 16. The 3-D printed K-band horn antenna without lens obtained a gain between the range of 12 dBi to 16 dBi as presented in Figure 16 which illustrates a mutual agreement with the commercial horn antenna. For the 3-D printed Ka-band horn antenna without lens, the gain between the range of 12 dBi to 15 dBi was obtained. For the Ka-band horn antennas, the gain increased up to a maximum gain of 26.5 dBi with the use of lens as presented in Figure 16. There is an increase of 10 dBi for the gain when use the lens throughout the K-band and Ka-band frequency range. For the commercial horn antenna, the gain with lens is better than the gain without lens.

Use of lens allows narrowed beamwidth which focus signals in particular direction throughout the K-band frequency range by converting the spherical waves to plane waves. The more focused the radio waves are, the higher the antenna gain. The higher the dBi value of the antenna, the greater the gain but the narrower the field pattern, implying that the signal power will go further in narrower direction.

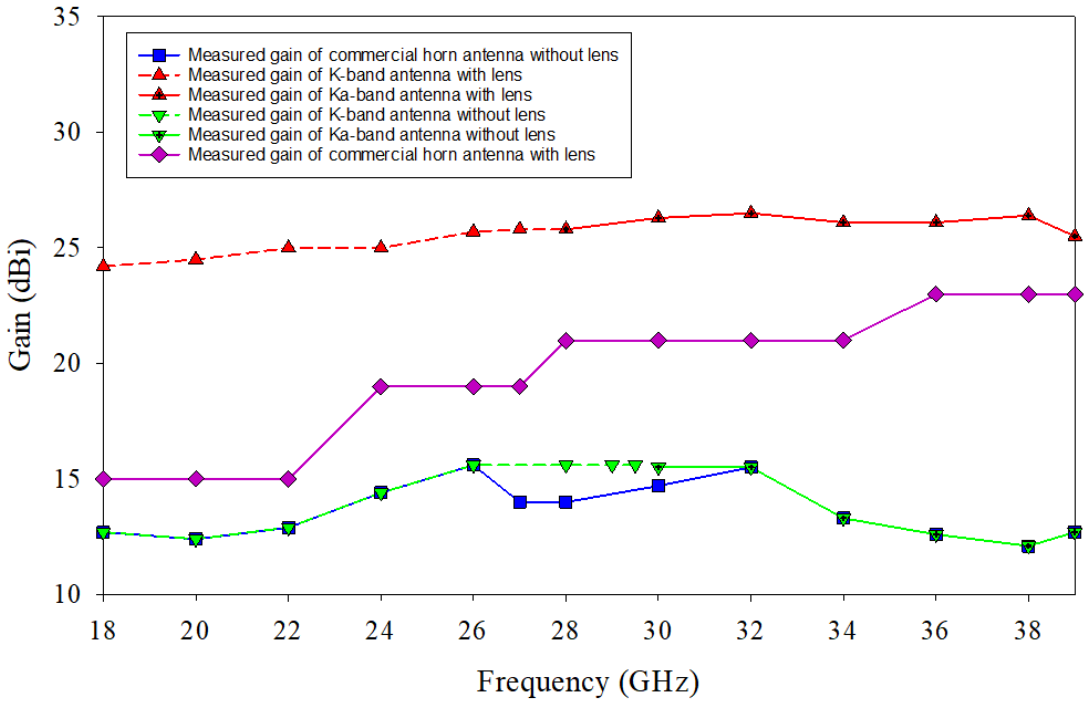

Fig. 16. Gain of K-band antenna with and without lens

4.4 Comparison of Software Results For 3-D Printed Horn Antennas and Commercial Horn Antenna

The dielectric properties of various materials could be measured as the size of free space material measurement system and area of the MUTs are small and hence practically feasible. The dielectric lens can precisely focus the E-field to fit the beam size and allows narrowed beamwidth which focus signals in particular direction which allows accurate determination of materials' permeability and permittivity. The researcher proved that dielectric characterization of materials may be accomplished using an in-house made FS measurement device in conjunction with a developed analytical extraction approach by determining the correct root through extracted results, removing the need for costly commercial measurement systems and software. In this study, we conducted tests on eight samples measuring 5 mm in thickness and having dimensions of 100 mm × 100 mm. These samples were polycarbonate (PC), polyvinyl chloride (PVC), polypropylene (PP), FR4, ABS, epoxy, Teflon and acrylic.

As frequency rises, the dielectric constant becomes non-linear and loses value more quickly. The loss of electric power rises at high frequencies. For high frequency applications, materials with low dielectric constant values are recommended for this reason among others. At higher frequencies, the polarisation process stops causing the dielectric to become polarised because the charge movement cannot keep up with the alternating field. The material's dielectric constant decreases with increasing frequency because each polarisation mechanism stops contributing, resulting in a decrease in the material's net polarisation [18-20]. Usually, the dielectric constant has a frequency dependence, meaning that its value increases at lower frequencies and decreases at higher frequencies. The molecules have more time to align and polarise at lower frequencies, but not enough time at higher frequencies. These corresponds to the decrease in dielectric constant value as the frequency increases. Table 6 presents the dielectric constant of the MUTs at GHz frequency. Dielectric properties determination is necessary in our daily life applications such as in cooking oil and dielectric fluid [21,22].

The permeability decreases to a considerably smaller amount at higher frequencies due to the fact known as the "skin effect," which is the inability of the magnetic field to pass through the core

or the interior of the lamination. At lower frequencies, the changes are negligible. As frequency, conductivity, and magnetic permeability increase, the depth of penetration decreases. These contributes to the decrease in permeability value as frequency increases. Table 6 shows the permeability of the MUTs at GHz frequency.

Table 6
MUTs dielectric constant at GHz frequency [18-20]

Type of MUTs	Dielectric constant at GHz	Permeability at GHz
FR4	4.5	~1
Polypropylene	2.2	~1
ABS	2.39	~1
Polycarbonate	2.8	~1
PVC	2.7	~1
Acrylic	2.9	~1
Teflon	2.1	~1
Epoxy	4.0	~1

The software was employed to generate plots showcasing the permittivity and permeability outcomes for the MUTs in relation to the K-band, Ka- band and commercial horn antennas. The ensuing visualizations, presented in Figure 17, depict the permittivity outcomes for FR4 material, both with and without the incorporation of a lens. Notably, the permittivity value for FR4 material is situated within the range of 4.5. Furthermore, it is discerned that the utilization of a lens has a positive impact on the permittivity of FR4, rendering it superior to the permittivity value observed in the absence of a lens. The permittivity of FR4 with the use of lens is better than the permittivity obtained without the use of lens as the dielectric lens can precisely focus the E-field to fit the beam size. The permittivity obtained with the use of lens is close to the original permittivity value of FR4.The permittivity of FR4 would be 4.5 as in Figure 4.30. The graph of permittivity with lens was good compared with the graph of permittivity without the lens for the FR4 for the K-band, Ka-band and commercial horn antennas.

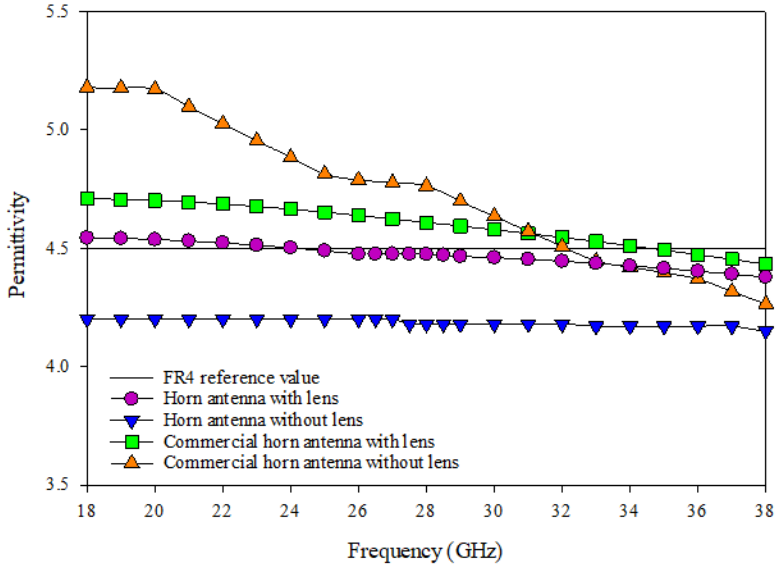

Fig. 17. ε_r of FR4 with and without lens

As for the permeability of FR4, value nearer to 1 were obtained with and without use of lens as in Figure 18. When compared to the permeability achieved without the lens, the permeability for FR4 with the lens is more desirable.

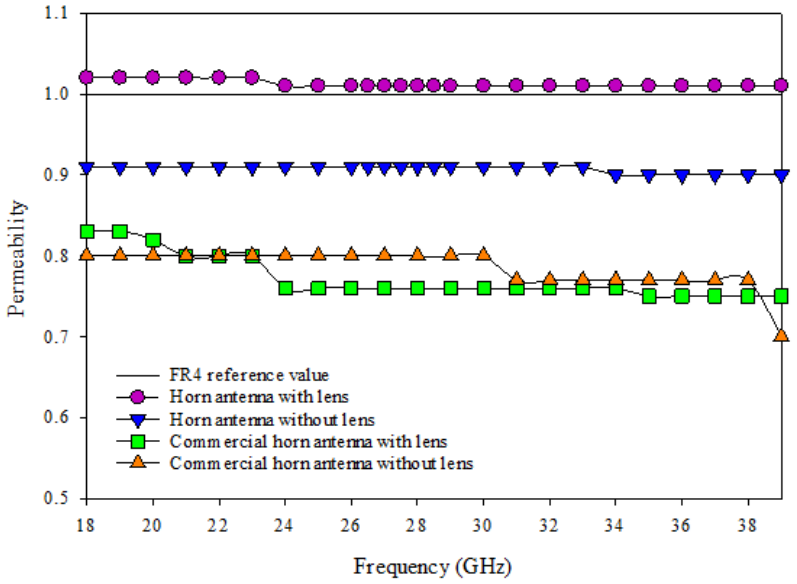

Fig. 18. μ_r of FR4 with and without lens

For the polypropylene the permittivity would be from 2.2. Figure 19 below shows the permittivity of polypropylene with and without lens. The permittivity of the polypropylene retrieved with the lens ranged nearer to 2.2, which corresponded to the original permittivity value of polypropylene.

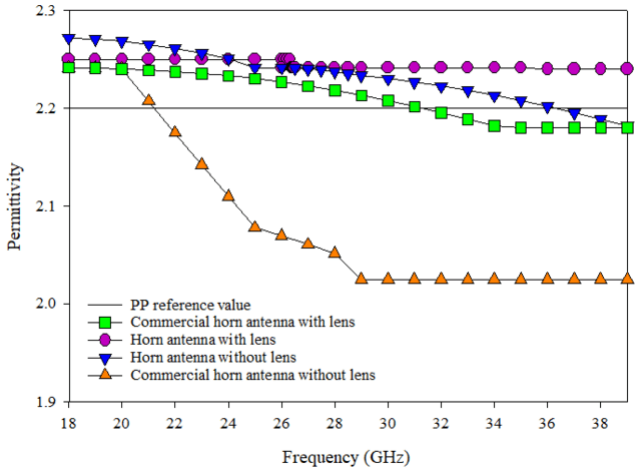

Fig. 19. Ɛr of polypropylene with and without lens

As for the permeability of polypropylene, the value is approximate to 1 with and without lens as in Figure 20. In line with the figure, the permeability for polypropylene accomplished with lens is greater with lens use, which is approximately 1.

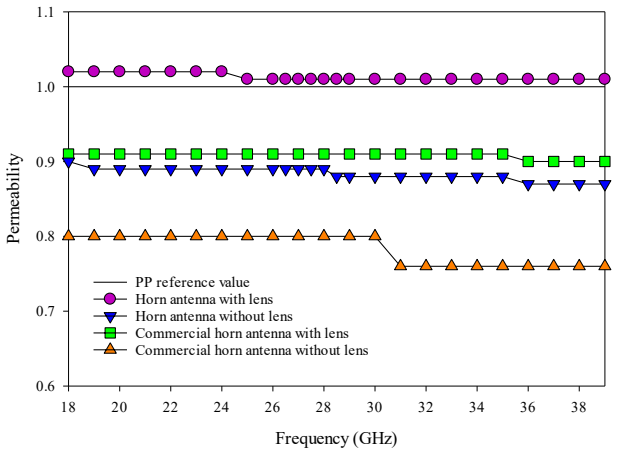

Fig. 20. μr of polypropylene with and without lens

The permittivity of ABS is in the range of 2.39. The permittivity of ABS with and without lens was shown in Figure 21. The graph curve with lens is good compared to the graph curve without lens.

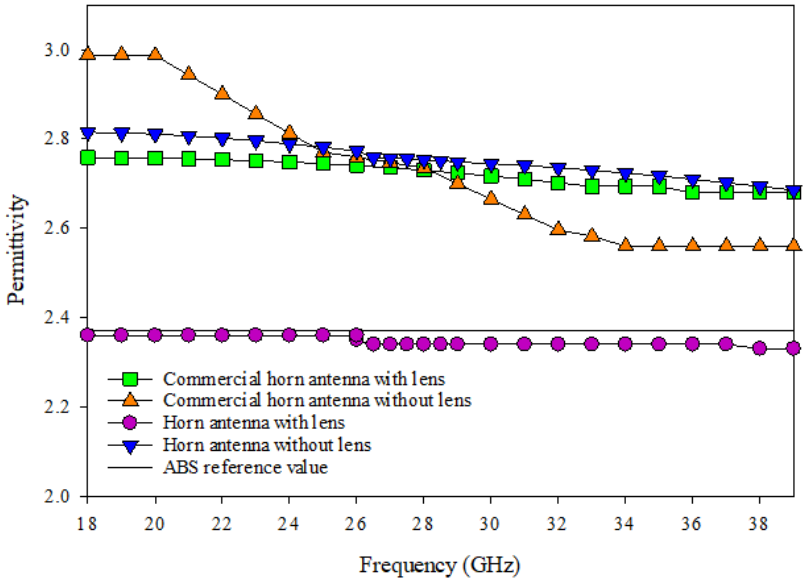

Fig. 21. Ɛr of ABS with and without lens

As for the permeability of ABS, the value nearer to 1 were acquired with and without use of lens as in Figure 22. According to the figure, the permeability attained for ABS with the lens is better which is close to 1.

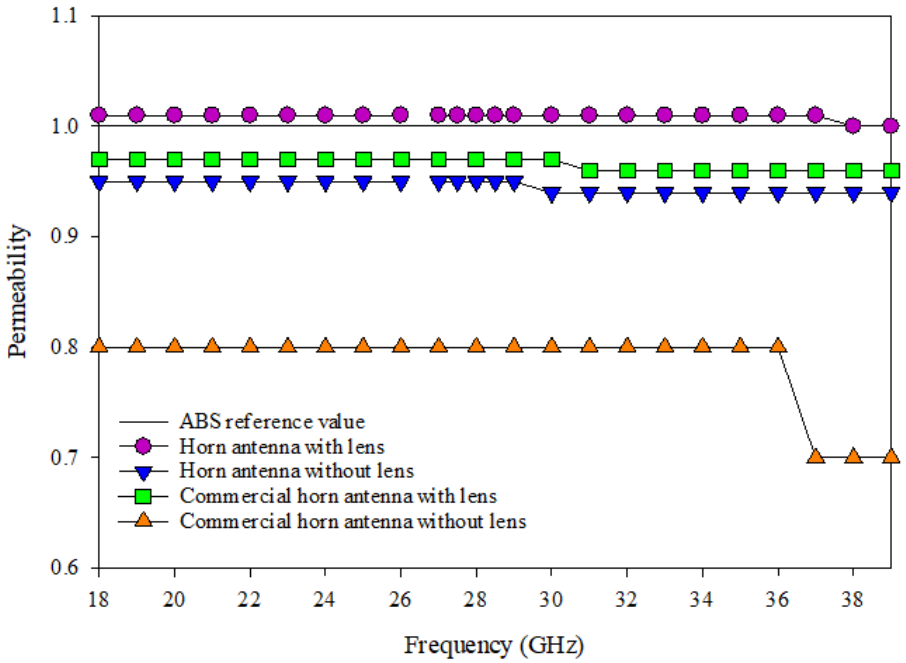

Fig. 22. μ_r of ABS with and without lens

Besides for the polycarbonate material, the permittivity is in the range of 2.8 as presented in Figure 23. With the use of lens, smooth graph of permittivity for polycarbonate was obtained when compared with the graph of permittivity without the use of lens.

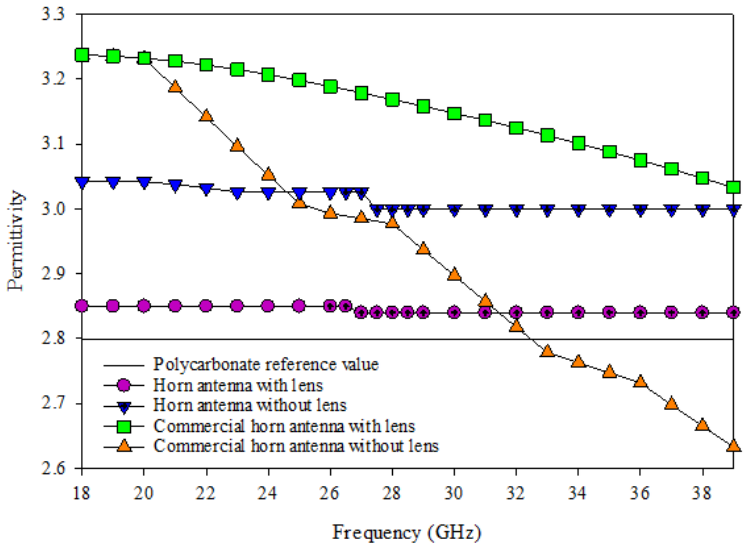

Fig. 23. Ɛr of polycarbonate with and without lens

As for the permeability of polycarbonate, the value approximate to 1 were obtained with and without lens as in Figure 24. According to the graph, the permeability of polycarbonate achieved with lens improves with lens use, and it is approximately 1.

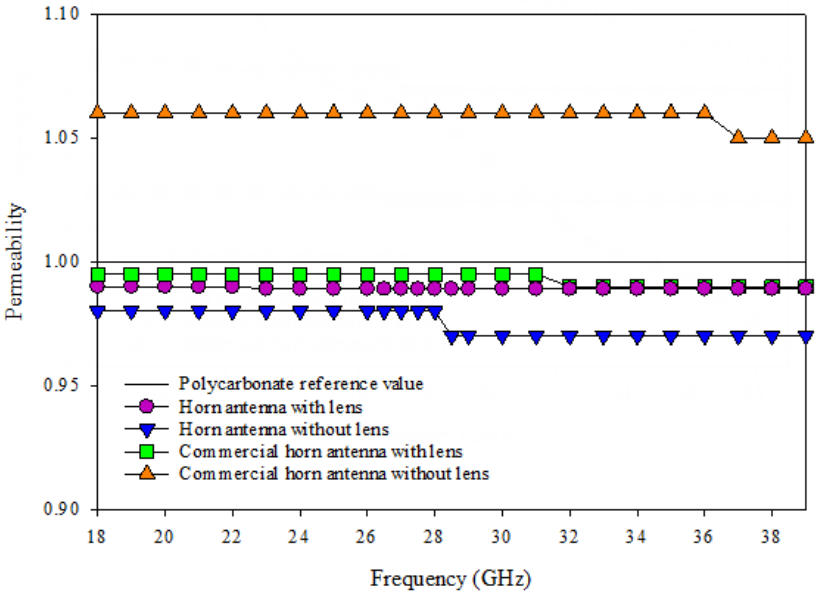

Fig. 24. μ_r of polycarbonate with and without lens

Also, for the PVC the permittivity is in the range of 2.7. As can be seen form Figure 25, the permittivity acquired were in the range of 2.7 with the use of lens. Smooth curve of permittivity was obtained with use of lens.

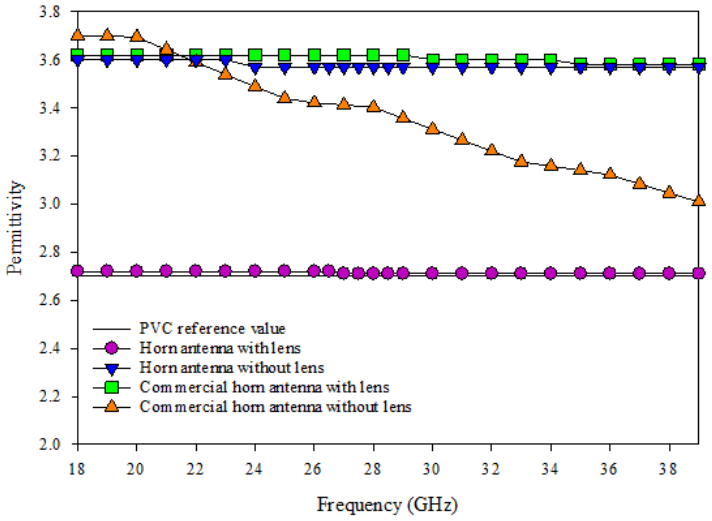

Fig. 25. Ɛr of PVC with and without lens

As for the permeability of PVC, the value obtained were nearer to1 as can be seen from Figure 26. The permeability recorded for PVC with lens is substantially greater than the permeability obtained without lens, according to the figure.

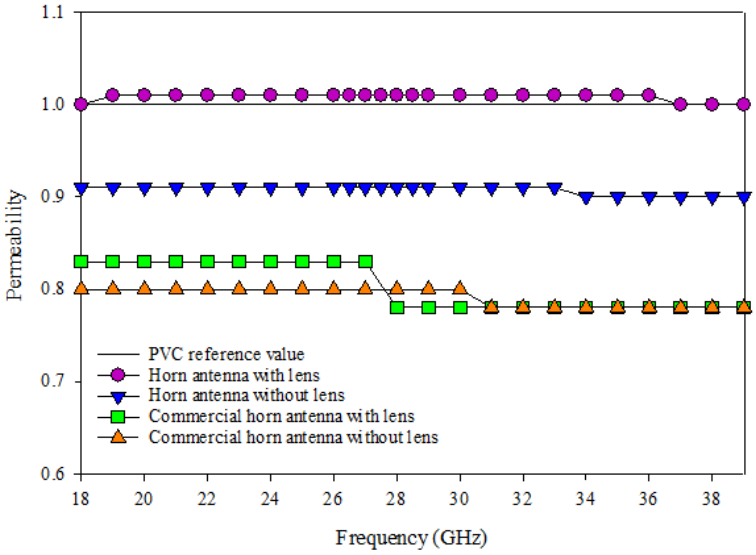

Fig. 26. μ_r of PVC with and without lens

For the acrylic the permittivity is in the range of 2.9. Smooth graph of permittivity was obtained with the lens when compared to the graph without lens as in Figure 27. The permittivity of the acrylic obtained with the lens ranged 3.0, which closer to the acrylic's original permittivity value.

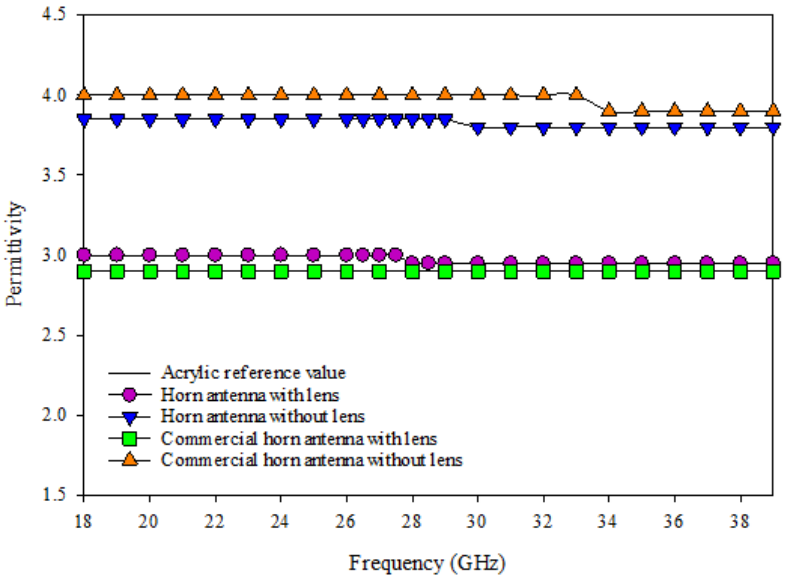

Fig. 27. Ɛr of acrylic with and without lens

As for the permeability of the acrylic, the value obtained were nearer to 1 with and without lens as can be seen from Figure 28. According to the graph, the use of a lens enhances the permeability of acrylic, which is near to 1.

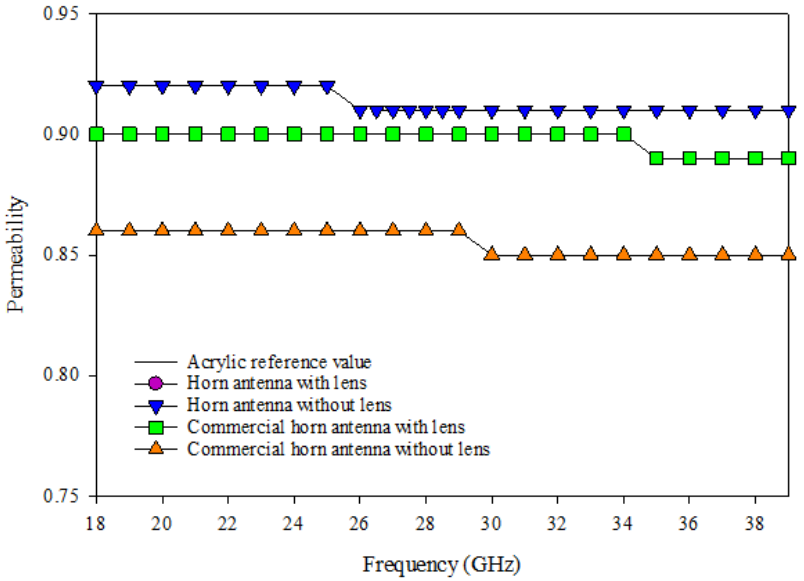

Fig. 28. μ_r of acrylic with and without lens

For Teflon the permittivity is 2.1. Figure 29 shows the permittivity of Teflon with and without lens. With the use of lens, a smooth curve of permittivity was obtained when compared to the curve without lens. When compared to the graph of Teflon permittivity without the use of a lens, a smooth graph of Teflon permittivity in the range nearer to 2.1 to was achieved with the use of a lens.

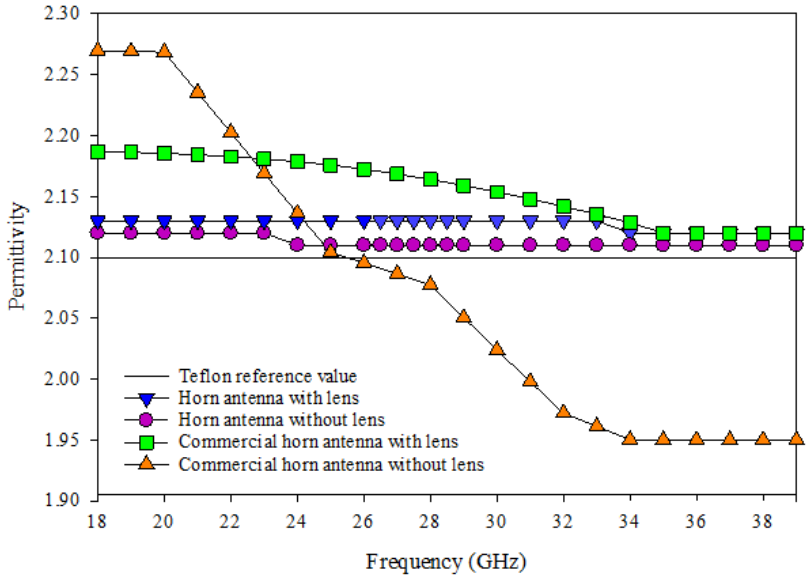

Fig. 29. Ɛr of Teflon with and without lens

The permeability of Teflon with and without lens were nearer to 1 as can be seen from Figure 30. According to the graph's findings, using a lens improves Teflon's permeability to a number closer to 1.

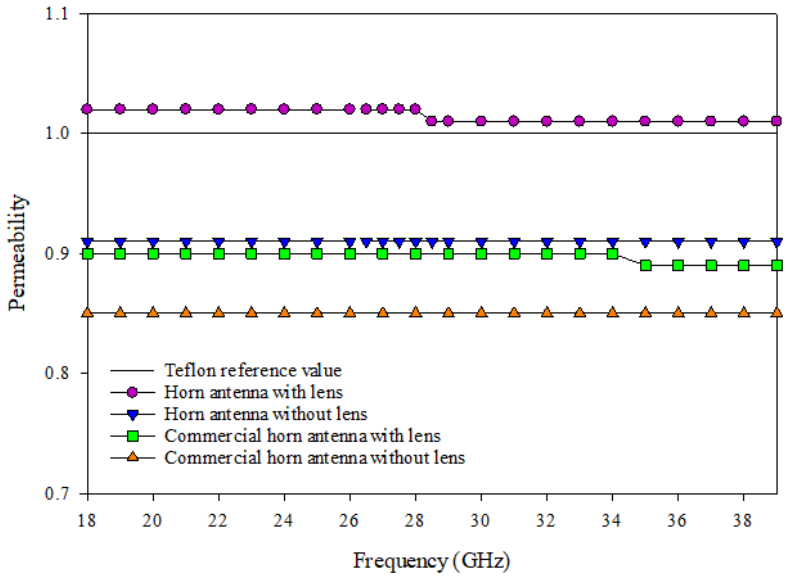

Fig. 30. μ_r of Teflon with and without lens

For the epoxy, the permittivity is in the range of 4. Figure 31 below shows the permittivity of epoxy with and without lens. A smooth graph of permittivity was acquired through the use of lens when compared with the graph without lens. With the aid of a lens, the epoxy's predicted permittivity, which was closer to 4, was established.

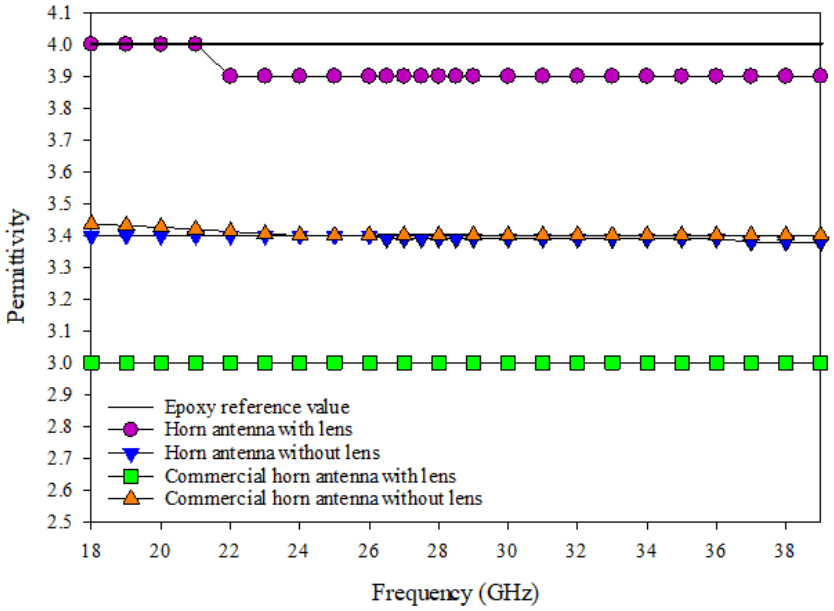

Fig. 31. Ɛr of epoxy with and without lens

As for the permeability of epoxy, the value obtained were approximate to1 as shown in Figure 32 with and without use of lens. According to the graph's results, using a lens enhances epoxy's permeability to a value that is closer to 1.

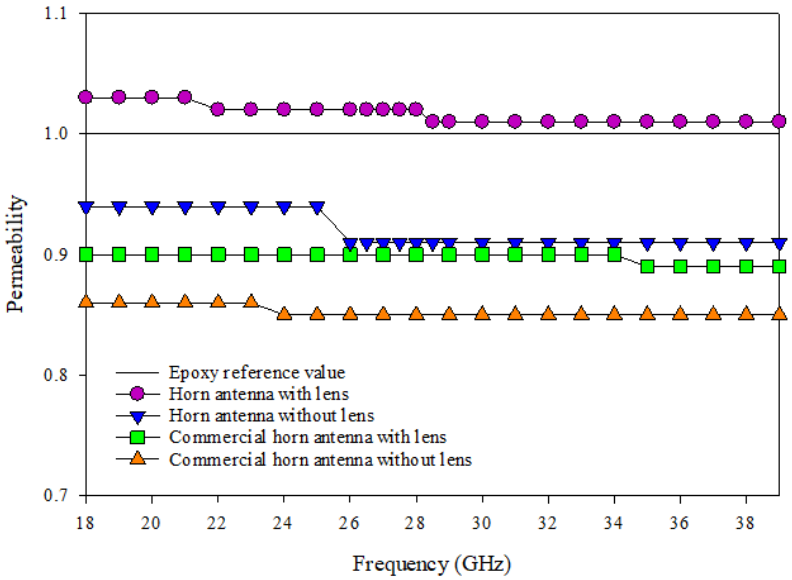

Fig. 32. μ_r of epoxy with and without lens

5. Conclusions

A notable contribution stems from the utilization of 3-D printing technology in crafting horn antennas and a dielectric lens. Upon comparative evaluation with the commercial horn antenna, the 3-D printed horn antennas exhibited good agreement across key performance parameters, encompassing S11, gain, and the 3-dB beamwidth. S_{11} below -10 dB was obtained for the 3-D printed horn antennas for K-band and Ka-band which showed a good agreement with S_{11} acquired by the commercial horn antenna. As for the 3- dB beamwidth, there is a difference of 10º to 20º between the commercial horn antenna and K-band and Ka-band horn antennas. For the gain, the commercial horn antenna acquired gain which is between the range of 13 dBi to 16 dBi for K-band and 13 dBi to 14.5 dBi for Ka-band. The 3-D printed K-band and Ka-band horn antennas obtained a gain between the range of 12 dBi to 16 dBi which illustrates a mutual agreement with the commercial horn antenna.

The successful implementation of this dielectric lens yielded tangible improvements, including higher gain and a reduction in beamwidth. These advancements collectively facilitated beam focusing, enabling the horn antenna to achieve more precise and controlled electromagnetic signal concentration. For the K-band horn antenna, without the use of lens, 3- dB beamwidth is in the range of 33º to 41.5º while with the use of lens, the 3- dB beamwidth is in the range of 8.9º to 9.7º. Use of lens allows narrowed beamwidth which focus signals in particular direction throughout the K-band frequency range. As for the gain, with the use of lens the gain increased with a maximum gain of 25.7 dBi at 26 GHz when compared to the gain without the use of lens with a maximum gain of 15.6 dBi at 26 GHz. As for the Ka-band horn antenna, without the use of lens, 3- dB beamwidth is in the range of 28º to 50º while with the use of lens, the 3- dB beamwidth is in the range of 7º to 9º. Also, for the gain, with the use of lens the gain increased with a maximum gain of 26.5 dBi at 32 GHz when compared to the gain without the use of lens with a maximum gain of 15.5 dBi at 32 GHz.

The software made through modified NRW algorithm also able to determine the permeability and permittivity of materials such as polycarbonate (PC), polyvinyl chloride (PVC), polypropylene (PP), FR4, ABS, epoxy, Teflon and acrylic precisely. These proves that the use of dielectric characterization of materials can be accomplished using an in-house created free space measurement system in conjunction with a developed analytical extraction approach. A dedicated software program capitalizes on the advanced NRW algorithm to achieve exact and finely detailed

assessments of permeability and permittivity was developed as well. This innovative software addition enhances the ability to discern these fundamental electromagnetic properties with a heightened level of accuracy and resolution. This program is tailored for both the 3-D printed horn antennas and the conventional commercial horn antenna. Both the permittivity and permeability of K-band, Ka-band and commercial horn antennas were determined accurately through this software program. The permeability and permittivity results of the MUTs even better with the use of lens.

The goal of this research is to create a free space material measurement system that can accurately determine permeability and permittivity by utilising the 3-D printed horn antennas, dielectric lens and software.

Acknowledgement
This research was supported by the Malaysian Technical Universities' Network (MTUN) Matching Research Grant, which was awarded by the Ministry of Higher Education of Malaysia (MOHE) under Project No. UniMAP/PPPI/GRN IRPA/MTUN/9002-00101/9028-00016. This research also was supported by Universiti Malaysia Perlis (UniMAP).

References

[1] Automatic RF Techniques Group, IEEE Microwave Theory and Techniques Society, and Institute of Electrical and Electronics Engineers. n.d. *RF to Millimeter-Wave Measurement Techniques for 5G and beyond 2020 94th ARFTG Microwave Measurement Conference: January 26th-29th, 2020, Grand Hyatt San Antonio, San Antonio, Texas*.

[2] Brinker, Katelyn, Matthew Dvorsky, Mohammad Tayeb Al Qaseer, and Reza Zoughi. "Review of advances in microwave and millimetre-wave NDT&E: Principles and applications." *Philosophical Transactions of the Royal Society A* 378, no. 2182 (2020): 20190585. https://doi.org/10.1098/rsta.2019.0585

[3] Cai, Linhong, Hu Zheng, Yihang Tu, and Yong Gao. "Wide band dielectric measurement technology with variable temperature based on free space method." In *2022 International Conference on Microwave and Millimeter Wave Technology (ICMMT)*, pp. 1-3. IEEE, 2022. https://doi.org/10.1109/ICMMT55580.2022.10022969

[4] Chen, Lihua, Chiho Kim, Rohit Batra, Jordan P. Lightstone, Chao Wu, Zongze Li, Ajinkya A. Deshmukh et al. "Frequency-dependent dielectric constant prediction of polymers using machine learning." *npj Computational Materials* 6, no. 1 (2020): 61. https://doi.org/10.1038/s41524-020-0333-6

[5] Ismail, Nurul Hidayah, and Mariatti Mustapha. "A review of thermoplastic elastomeric nanocomposites for high voltage insulation applications." *Polymer Engineering & Science* 58, no. S1 (2018): E36-E63. https://doi.org/10.1002/pen.24822

[6] Jandyal, Anketa, Ikshita Chaturvedi, Ishika Wazir, Ankush Raina, and Mir Irfan Ul Haq. "3D printing–A review of processes, materials and applications in industry 4.0." *Sustainable Operations and Computers* 3 (2022): 33-42. https://doi.org/10.1016/j.susoc.2021.09.004

[7] Karol, Vidushi, Chandra Prakash, and Anshu Sharma. "Observation of high dielectric properties of Mg-substituted BST ceramic synthesized by conventional solid-state route." *Journal of Materials Science: Materials in Electronics* 32, no. 14 (2021): 19478-19486. https://doi.org/10.1007/s10854-021-06465-6

[8] Krupka, Jerzy. "Microwave measurements of electromagnetic properties of materials." *Materials* 14, no. 17 (2021): 5097. https://doi.org/10.3390/ma14175097

[9] Kumar, Jitendra, Sagar Singh, Skand Tripathi, Vishal Shukla, and Shiva Pathak. "Design and fabrication of 3-axis CNC milling machine using additive manufacturing." *Materials Today: Proceedings* 68 (2022): 2443-2451. https://doi.org/10.1016/j.matpr.2022.09.145

[10] Lim, Sungmook, Choul-Young Kim, and Songcheol Hong. "Simultaneous measurement of thickness and permittivity by means of the resonant frequency fitting of a microstrip line ring resonator." *IEEE Microwave and Wireless Components Letters* 28, no. 6 (2018): 539-541. https://doi.org/10.1109/LMWC.2018.2833202

[11] Michalak, Joanna, Marta Czarnowska-Kujawska, Joanna Klepacka, and Elżbieta Gujska. "Effect of microwave heating on the acrylamide formation in foods." *Molecules* 25, no. 18 (2020): 4140. https://doi.org/10.3390/molecules25184140

[12] Ozturk, Turgut, and Muhammet Tahir Güneşer. "Measurement methods and extraction techniques to obtain the dielectric properties of materials." *Electrical and Electronic Properties of Materials* 6 (2018): 83-108. https://doi.org/10.5772/intechopen.80276

[13] "PCB Design Considerations for MmWave | 2022-10-09 | Microwave Journal." n.d. Accessed January 31, 2023.

[14] Sato, Yasumoto, Natsuki Ogura, Yuhei Yamaguchi, and Yang Ju. "Development of a sensor for dielectric constant measurements utilizing time-domain measurement with a vector network analyzer." *Measurement* 169 (2021): 108530. https://doi.org/10.1016/j.measurement.2020.108530

[15] Semenenko, V. N., V. A. Chistyaev, A. A. Politiko, and K. M. Baskov. "Test stand for measuring the free-space electromagnetic parameters of materials over an ultrawide range of microwave frequencies." *Measurement Techniques* 62 (2019): 161-166. https://doi.org/10.1007/s11018-019-01601-5

[16] Sivakumar, Renukka, Yeng Seng Lee, Saidatul Norlyana Azemi, Zahari Awang Ahmad, Ping Jack Soh, and Kok Yeow You. "A Free-Space Measurement System for Microwave Materials at Kuband." In *2022 IEEE International RF and Microwave Conference (RFM)*, pp. 1-4. IEEE, 2022. https://doi.org/10.1109/RFM56185.2022.10064980

[17] Tlhabologo, Bokang Agripa, Ravi Samikannu, and Modisa Mosalaosi. "Alternative liquid dielectrics in power transformer insulation: a review." *Indonesian Journal of Electrical Engineering and Computer Science* 23, no. 3 (2021): 1761-1777. https://doi.org/10.11591/ijeecs.v23.i3.pp1761-1777

[18] Vohra, Nagma, and Magda El-Shenawee. "K-and W-band free-space characterizations of highly conductive radar absorbing materials." *IEEE Transactions on Instrumentation and Measurement* 70 (2020): 1-10. https://doi.org/10.1109/TIM.2020.3041821

[19] Wang, Ziye, Yang Yu, Lingbo Qiao, and Ziran Zhao. "Material Identification Using Dielectric Properties with Millimeter-wave Imaging System." In *2020 Cross Strait Radio Science & Wireless Technology Conference (CSRSWTC)*, pp. 1-3. IEEE, 2020. https://doi.org/10.1109/CSRSWTC50769.2020.9372690

[20] Wang, Renche, Hui Lv, Jiamin Zhai, and Tao Shen. "Research and Exploration of Terahertz Feeder Manufacturing Technology Based on Micro-precision Machining." In *Journal of Physics: Conference Series*, vol. 2459, no. 1, p. 012133. IOP Publishing, 2023. https://doi.org/10.1088/1742-6596/2459/1/012133

[21] Deraman, Muhammad Nazori, Norazhar Abu Bakar, Nur Hakimah Ab Aziz, and Imran Sutan Chairul. "The experimental study on the potential of waste cooking oil as a new transformer insulating oil." *Journal of Advanced Research in Fluid Mechanics and Thermal Sciences* 69, no. 1 (2020): 74-84. https://doi.org/10.37934/arfmts.69.1.7484

[22] Dzulkifli, Norazkifni Faizura, Azuddin Mamat, and Imtiaz Ahmed Choudhury. "The potential of water-in-oil emulsion of canola oil as dielectric fluid for EDM process." *Journal of Advanced Research in Fluid Mechanics and Thermal Sciences* 72, no. 2 (2020): 129-141. https://doi.org/10.37934/arfmts.72.2.129141